

Effect of External Forcing on Droplet Dispersion in a Developing Shear Layer

S. K. Aggarwal* and Y. Xiao†

University of Illinois at Chicago, Chicago, Illinois 60680

The dynamics and dispersion of nonevaporating droplets in a forced transitional shear layer are studied. The shear layer is formed by two coflowing parallel streams downstream of a splitter plate. The effects of periodic forcing on the dynamics of large-scale vortical structures and on the dispersion characteristics of droplets in a spatially and temporally developing shear layer are investigated. Results indicate that by forcing the shear layer at the first subharmonic of the fundamental mode, the droplet dispersion can be enhanced significantly. The forcing at the fundamental mode increases droplet dispersion in the initial part, but then decreases dispersion farther downstream. These results are consistent with the previously published experimental and numerical results on the effect of forcing on the shear layer growth. It is also observed that the forcing causes a relatively larger gain in dispersion for intermediate size particles compared to that for gas particles, implying that the centrifugal mechanism may be strengthened by forcing. The dispersion enhancement is more pronounced in the initial part of the shear layer, which is perhaps the more important region for improved droplet dispersion and mixing in spray applications.

Introduction

PARTICLE-LADEN turbulent flows occur in numerous technological and environmental systems. The traditional approach for modeling these flows is based on the assumption that the turbulence is isotropic and statistical in nature. The turbulent properties are then obtained from the average behavior of the turbulent carrier fluid by using the time- or Favre-averaged governing equations along with some semi-empirical turbulence models. The dispersed phase is represented by a large number of discrete particles, and their dynamic behavior is determined in a deterministic or a stochastic manner.

A number of experimental and computational studies,¹⁻⁷ published during the last two decades, have demonstrated that the turbulent flows, which previously were thought to be totally chaotic and statistical in nature, are dominated by large-scale coherent vortical structures. This has caused a major shift in thinking as to how the dynamics of turbulence be perceived and modeled. In fact, a number of important questions have been posed by these studies. How useful or relevant are the semi-empirical models based on the Reynolds- or Favre-averaged approach? To what extent are the mixing and entrainment processes influenced by the dynamics of organized structures? How is particle dispersion behavior affected by the large-scale structures, and in turn, how are these structures influenced by the dispersed phase? What are the effects of these structures on the gasification behavior of fuel droplets? How do the dynamic interactions between the large structures and droplets influence the fuel vapor distribution, and, consequently, the ignition, extinction, and combustion processes? Although the results reported in Refs. 1-7 have not provided satisfactory answers to these questions, they have seriously challenged the adequacy of the traditional approaches for accurately describing the turbulent two-phase flows.

Further interest in the study of large-scale structures stems from the fact that by manipulating these structures, one may be able to control and enhance the performance of systems whose dynamics is strongly influenced by these structures. The experimental investigations of a forced mixing layer by Ho and Huang⁸ and Oster and Wygnanski⁹ clearly indicate that the initial condition has a long-lasting effect on the development of the mixing layer. These studies further show that the spreading rate of the mixing layer can be manipulated by forcing at a subharmonic of the natural instability frequency. If the forcing can have such a strong effect on the dynamics of large-scale structures in a mixing layer, it is then natural to ask what influence does the forcing have on the dynamics of particles injected into the layer?

The present study investigates the effect of periodic forcing on dynamics and dispersion of nonevaporating droplets injected into a transitional shear layer. The purpose is to study both qualitatively and quantitatively what influence the forcing of the shear layer has on the dynamics of large-scale structures, and thereby on the dispersion characteristics of droplets. The investigation focuses on the initial development of a spatially developing shear layer, where the dynamics are controlled by large spanwise structures. In terms of energy spectrum, it implies that most of the energy is in large-scale structures. The effects of forcing frequency and amplitude are investigated first on the initial roll-up and vortex merging, and then on the dynamics and dispersion behavior of droplets. In this article, a two-dimensional shear layer is simulated. The effects of small-scale structures and other three-dimensional features on droplet dispersion are not considered. These assumptions are justified by the numerous experimental and computational investigations (following the classical experiments of Brown and Roshko¹) that demonstrate the persistence of spanwise structures over a large distance in the streamwise direction. In addition, some recent experimental studies^{6,7} clearly indicate that the droplet dispersion is mainly controlled by the large spanwise structures. The present study is aimed at examining how the dispersive action of these structures is modified by external forcing.

Previous works on mixing layer simulations have employed spectral,¹⁰ vortex dynamics,¹¹ and finite difference¹²⁻¹⁴ techniques. These studies have focused on the dynamics of large-scale structures in temporally developing mixing layer¹¹ and spatially developing layers.^{13,14} The former approach is com-

Received April 5, 1993; revision received Aug. 8, 1993; accepted for publication Aug. 9, 1993. Copyright © 1993 by S. K. Aggarwal and Y. Xiao. Published by the American Institute of Aeronautics and Astronautics, Inc., with permission.

*Associate Professor, Department of Mechanical Engineering, Associate Fellow AIAA.

†Graduate Student, Department of Mechanical Engineering.

putationally more efficient because of the relatively compact spatial domain. However, the spatially developing case more closely resembles laboratory as well as practical situations. In addition, this approach is able to capture some important features, such as asymmetric mixing,^{12,13} that are not predicted by the temporal approach. Previous studies on the particle dynamics in mixing layers have used the vortex dynamics^{16,17} as well as finite difference¹⁸ approaches for the gas phase, and a Lagrangian approach for the particles. However, none of the previous studies reported so far have investigated the influence of forcing on the particle dynamics and dispersion.

Physical Model

The shear layer considered in the present study is formed by two coflowing parallel streams downstream of a splitter plate. A schematic of the physical model is shown in Fig. 1. The computational domain is marked by a broken line. The droplets of given size and velocity are injected at specified cross-stream locations at the inflow boundary ($x = 0$).

The governing equations for the carrier fluid are the time-dependent, two-dimensional equations for the conservation of mass, momentum, and energy. The source terms appearing in these equations due to the exchange of mass, momentum, and energy with the dispersed phase are assumed negligible in the present study since the number of droplets considered is typically less than 2000. In other words, the droplets are influenced by the gas phase, but not vice versa. This is a reasonable assumption since the focus of this article is to examine how the dynamics of droplets is influenced by the large-scale structures in the initial region of a perturbed shear layer. Further details of the gas-phase equations are provided in Ref. 18.

The equations governing the dynamics of droplets can be written as

$$\frac{dX_p}{dt} = V_p \quad (1)$$

$$\frac{4}{3} \pi r_p^3 \rho_p \frac{dV_p}{dt} = F \quad (2)$$

where X_p and V_p are, respectively, the position and velocity vectors for a droplet represented by the subscript p , ρ_p is the material density of the dispersed phase, and r_p is the droplet radius. The force F in Eq. (2) is assumed to be due to the drag force on the particle. This implies that the contribution of the flow nonuniformities, flow acceleration, Magnus effect, and Basset history terms¹⁸ to F are negligible in comparison with the drag term. Based on a scale analysis, Lazaro and Lashearas⁷ found these contributions to be negligible. This is, however, not a limitation of the present study. Moreover, as discussed by Faeth,¹⁹ these terms can be neglected when $\rho_p/\rho \sim 10^3$. For the results presented here, $\rho_p = 1.0 \text{ gm/cm}^{-3}$

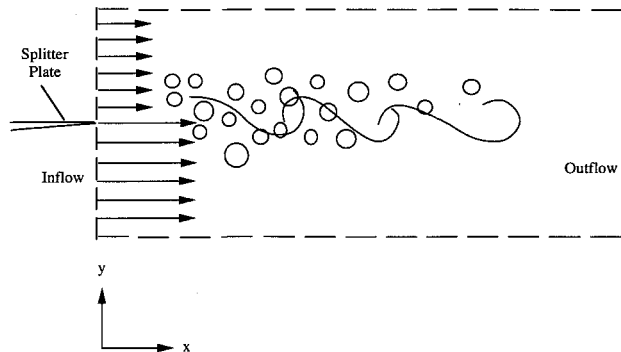


Fig. 1 Schematic of the physical model and the computational domain.

and the initial gas density is taken as $1.182 \times 10^{-3} \text{ gm/cm}^{-3}$. F is given by

$$F = C_d \frac{1}{2} \pi r_p^2 \rho |V - V_p| (V - V_p) \quad (3)$$

$$C_d = \frac{24}{Re_p} \left(1 + \frac{Re_p^{2/3}}{6} \right) \quad (4)$$

$$Re_p = \frac{2\rho |V - V_p| r_p}{\mu} \quad (5)$$

where the drag coefficient C_d is assumed to be given by the solid sphere drag correlation.¹⁹

Boundary Conditions

The free slip boundary conditions are specified at the top and bottom boundaries of the computational domain. At the left boundary, the inflow density and velocity are specified, and the pressure is allowed to float by employing a zero-gradient condition. This implies that the pressure at the guard cell, which is just outside the inflow boundary, is determined by the pressure at the first internal cell. As discussed by Grinstein et al.,¹² this allows the pressure at the inflow to adjust to the disturbances arriving from downstream, and the feedback mechanism to retrigger the instability. A step function as well as hyperbolic-tangent velocity profiles were used at the inflow boundary. The dynamics of large-scale structures as well as droplet dispersion behavior were found to be relatively insensitive to these velocity profiles.

A periodic forcing of the streamwise velocity component is employed to perturb the shear layer. The velocity boundary condition at the left boundary is then specified as

$$V_x = V_0(y) \left[1 + \sum_{m=1}^M a_m \sin(w_m t) \right] \quad (6)$$

where $V_0(y)$ is the streamwise velocity at the left boundary for the unperturbed case, and M specifies the number of forcing frequencies used.

In the present investigation, a single forcing frequency is used, i.e., $M = 1$. The forcing frequency is related to the natural instability (roll-up) frequency of the shear layer as

$$w_n = (1/n)(2\pi f) \quad (7)$$

where n is an integer. Note, for example, $n = 2$ corresponds to a forcing at the first subharmonic of the fundamental mode of the shear layer. Thus, the effect of forcing is considered by imposing a sinusoidal perturbation of a fixed frequency ω_1 and relative amplitude a_1 on the inflow axial velocity profile which is time-independent for the unforced case. The effects of forcing amplitude and frequency on the dynamics of large-scale structures and droplet dispersion are discussed in the next section.

A subsonic flow simulation requires a special treatment of the boundary conditions at an outflow boundary. The zero-gradient boundary conditions are employed for the density and velocities. The pressure at the guard cell, which is one grid length downstream of the last computational cell, is calculated by using

$$p_g = p_n + (X_g - X_n)(p_{\text{amb}} - p_n)/(X_g - X_0) \quad (8)$$

where the subscripts g and n refer to the guard cell and the last cell in the computational domain, respectively. X is the location of the inflow boundary, and p_{amb} is the pressure far away from the outflow boundary. The above equation is obtained by interpolating the pressure values p_n and p_{amb} . Additional discussion regarding this boundary condition and the

effects of outflow boundary conditions, in general, can be found in a more recent study by Grinstein.²⁰

The initial conditions for integrating the droplet equations involve the specification of X_p and V_p at a specified initial time. The initial droplet velocity is assumed to be the same as that of the slow gas stream. Note, however, that the dispersion behavior was found to be the same as the initial droplet velocity is varied between the slow-stream and fast-stream velocities. The initial X position for all the droplets is the inflow boundary, i.e., $X_p = 0$, whereas the initial Y position is varied in a parametric manner. For the base case, five cross-stream injection locations are specified. This means that starting at a given initial time, five droplets are injected with a specified frequency. The dynamics and dispersion behavior of these particles is then computed by numerically solving Eqs. (1) and (2). Note that the solution of these equations is coupled dynamically with that of the gas-phase equations that are also being solved simultaneously.

Numerical Procedure

The numerical scheme to solve the two-phase equations is based on a Eulerian-Lagrangian formulation. The algorithm to solve the Eulerian gas-phase equations is based on the flux corrected transport (FCT) methodology.¹² The particle equations are integrated using a second-order Runge-Kutta procedure. The generic algorithm employing the FCT procedure has been tested extensively for large-scale simulations of both nonreacting and reacting flows. It employs a time-step splitting, monotone, finite difference technique. Since the code is based on the solution of a one-dimensional conservation equation, a direction-splitting technique is employed for multidimensional computations. It is important to note that the FCT algorithm, in the present study, is used to resolve the large-scale features of the flow in the transitional region of the shear layer. As discussed by Boris et al.,²¹ the FCT approach is similar to large eddy simulation (LES) with implicit (built-in) subgrid models, and may be termed as monotone integrated large eddy simulation (MILES). Numerical evidence as well as physical arguments are presented by Boris et al. to calibrate MILES for large eddy simulation.

Starting at time $t = 0$, the gas-phase equations are integrated to simulate the dynamics of large-scale vortical structures. At a specified time during this simulation, the droplet injection is started. The droplets' trajectories are tracked by solving Eqs. (1) and (2) by using a second-order Runge-Kutta method. Note that the particle locations in general do not coincide with the fixed gas-phase grid points. A two-dimensional interpolation is employed to calculate the gas-phase properties, such as velocities and density which appear in Eqs. (3) and (4), at the instantaneous droplet locations.

Discussion of Results

The physical model used for shear layer simulation is shown in Fig. 1. The splitter plate is located upstream of the left boundary at $y = 3.0$ cm. Two coflowing streams, which form the shear layer, are assumed to initially have the same temperature and density. For the base case, the slow stream is at the top and has a velocity of 20.0 m/s. The fast stream has a velocity of 100.0 m/s. Note that the gas-phase algorithm used in this study has been well tested previously by Grinstein et al.²⁰ and shown to reproduce the large-scale features of a variety of flows that are observed in the laboratory experiments. This includes the Strouhal number for the shear layer roll-up and vortex mergings, the spatial distribution of merging locations, and the shear layer growth rate. We also conducted an independent study²² to further establish the credibility of numerical results, and computed several cases, varying the mean velocity (Reynolds number), velocity ratio, and initial momentum thickness. The predicted Strouhal number for all these cases ranged between 0.023–0.027, which is in good agreement with the experimentally observed range 0.025–0.031 reported by Hussain and Hussain.²³

Effect of Forcing on the Dynamics of Large-Scale Structures

The first part of the study focuses on the dynamics of the unforced shear layer in order to identify the optimum frequency for perturbing the shear layer. The experimental results of Ho and Huang⁸ and Oster and Wygnanski⁹ suggest that the subharmonic forcing of the shear layer produces the optimum enhancement in the rate of shear layer growth. To obtain the dominant frequencies in the unforced shear layer, the frequency spectra of the time-history of axial velocity recorded at several streamwise stations is obtained. For the

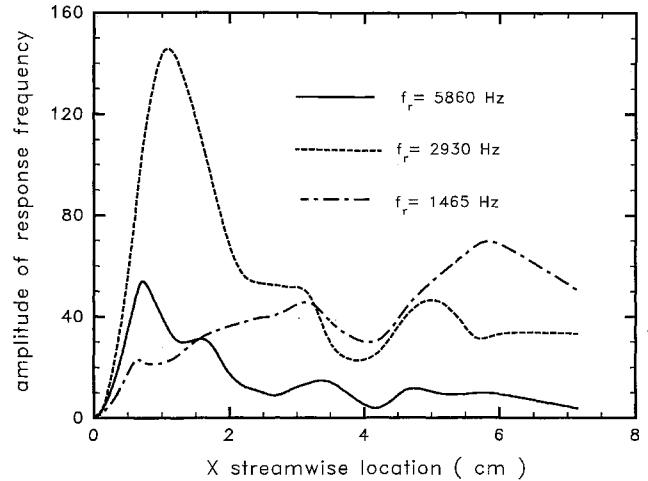


Fig. 2 Streamwise evolution of the amplitude of the roll-up, first merging, and second merging frequencies for the unperturbed shear layer.

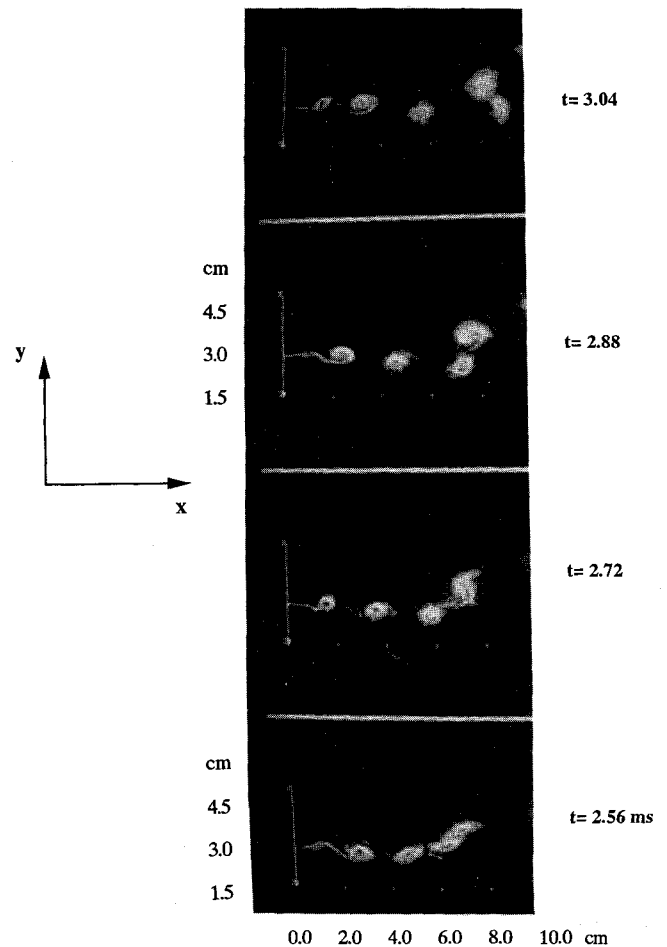


Fig. 3 Vorticity contours at $t = 2.56, 2.72, 2.88, 3.04$ ms for the unperturbed shear layer.

spectral analysis, the axial velocity is recorded starting at $t = 2.4$ ms, when the initial transients have become negligible. The total time used in the time series contains at least 24 roll-ups, and the frequency resolution in the spectral analysis is 244 Hz, which represents an error of 4.1% based on the roll-up frequency. From the detailed spectral analysis, the dominant frequencies are observed to be 5860, 2930, and 1465 Hz, which correspond, respectively, to the natural instability (roll-up), first merging, and second merging frequencies. The streamwise evolution of the amplitudes of these frequencies is shown in Fig. 2. The amplitude of 5860-Hz frequency peaks at $x = 0.8$ cm downstream of the splitter plate, implying that the shear layer roll-up occurs at this location. Similarly, $x = 1.1$ cm and $x = 6.0$ cm, where the 2930- and 1465-Hz frequencies attain their peak amplitudes, correspond to the first and second pairing locations, respectively. These locations are further confirmed by the vorticity contour plots shown in Fig. 3. For example, the plot at $t = 2.56$ ms shows the second pairing location at 6.0 cm, whereas the plot at $t = 2.72$ ms shows the first merging location at about 1.2 cm. Note that the first merging is observed to occur very close to the roll-up location. Further details of the spectral analysis and flow visualization are provided in Ref. 22.

The effect of forcing frequency on the streamwise evolution of the spectral characteristics of large-scale vortical structures is portrayed in Fig. 4. For these results, the forcing amplitude is maintained at a constant value of 1%, i.e., $a_m = 0.01$ in Eq. (6). Figures 4a, 4b, and 4c show, respectively, the streamwise evolution of the fundamental mode (5860 Hz), the first subharmonic, and the second subharmonic for the unperturbed

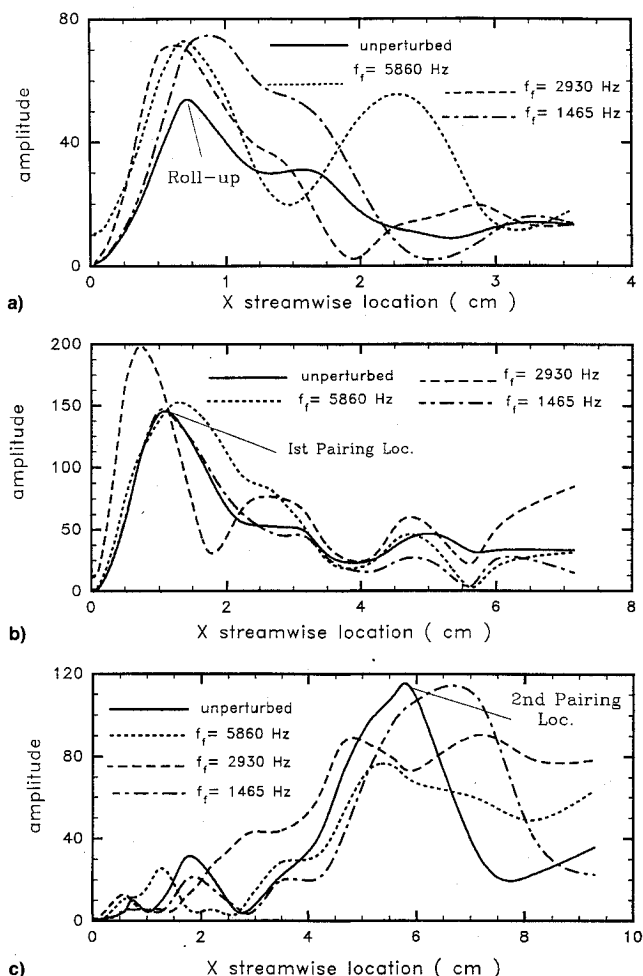


Fig. 4 Amplitude evolution of the roll-up frequency a) first merging frequency, b) second merging frequency, and c) for the unperturbed and perturbed shear layers with forcing frequency as a parameter. Forcing amplitude = 1%.

turbed and perturbed shear layer. For the latter, the forcing frequencies are 5860, 2930, and 1465 Hz. The important observation is that by forcing at the first subharmonic frequency ($f_f = 2930$) can yield a beneficial effect on the dynamics of the shear layer. As clearly indicated by the amplitude evolution of 5860- and 2930-Hz frequencies in Figs. 4a and 4b, respectively, it causes the shear layer roll-up and the first pairing to occur earlier compared to the unperturbed case. However, the second vortex pairing seems to be delayed due to this forcing. Also, forcing the shear layer at its fundamental or at second subharmonic frequency does not seem to produce any apparent desirable effect, i.e., the shear layer growth rate does not seem to be enhanced by forcing at these frequencies. The implication here is that the optimum forcing frequency for enhancing the droplet dispersion may correspond to the first subharmonic frequency. This is confirmed by the dispersion results presented in the next section.

Effect of Forcing on Droplet Dispersion

The droplet dynamics and dispersion behavior is studied by simulating a continuous injection of droplets from the upstream boundary. The droplet injection is started at time = 4.8 ms. By this time, the initial flow transient is out of the computational domain and the shear layer exhibits a quasi-periodic behavior. For the base case, the injection process is simulated over a period of 2.0 ms. This corresponds to about 12 shear layer roll-ups, and typically 1000–2000 droplets are injected during this time.

The effects of forcing the shear layer at different frequencies and amplitudes on droplet dispersion are characterized in terms of the dispersion function which is defined as

$$D(t, N) = \left[\sum_{i=1}^N (Y_i(t) - Y_{i0})^2 / N \right]^{1/2} \quad (9)$$

where N is the number of droplets in the flowfield at time t , Y_i the transverse location of a droplet at time t , and Y_{i0} the initial transverse location of the same droplet at the inflow

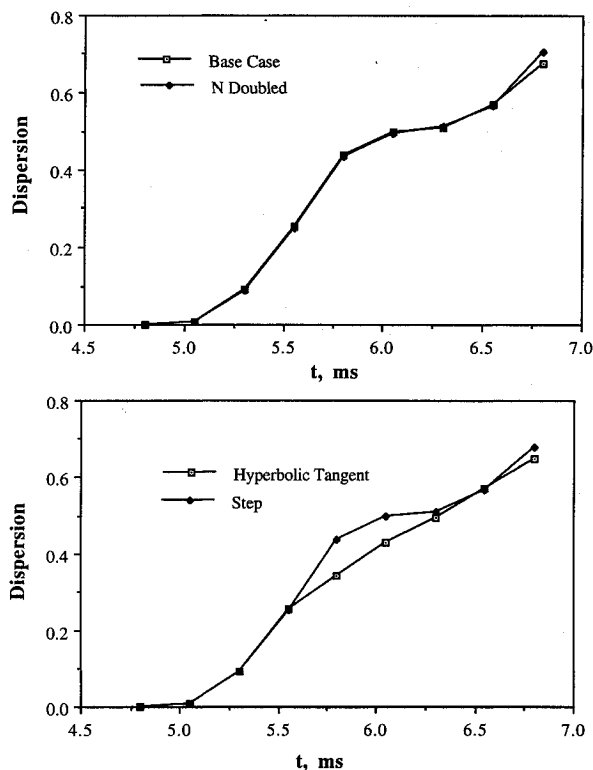


Fig. 5 Effect of the total number of droplets and inflow gas velocity profile on the dispersion function for the unperturbed shear layer. Droplet diameter = 5 μ m.

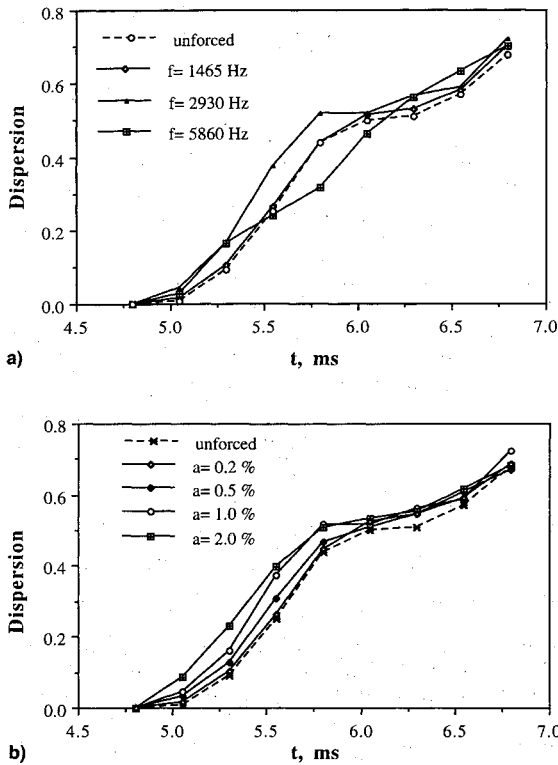


Fig. 6 Variation of droplet dispersion function with time for a) different forcing frequencies and b) amplitudes. The droplet diameter is 5 μm . The forcing amplitude is 2% in a), and the forcing frequency is 2930 Hz in b).

boundary. The temporal variation of the dispersion function for four different cases is given in Fig. 5. The important observation is that the droplet dispersion statistics are not sensitive to the number of droplets employed in the simulation. In addition, it is shown that the droplet dispersion behavior is relatively insensitive to the inflow gas velocity profiles.

Figure 6 shows the effect of the forcing frequency and amplitude on the dispersion of 5- μm diam droplets. The droplet Stokes number,²⁴ defined as the ratio of droplet response time to the characteristic flow time, for a 5- μm droplet is 0.45. The droplet response time is defined as $t_p = \rho_p d_p^2 / (18\mu)$, where ρ_p is the droplet material density, d_p the droplet diameter, and μ the viscosity of the carrier fluid. The characteristic flow time is based on the shear layer roll-up frequency. The important observation from Fig. 6a is that the droplet dispersion can be significantly enhanced by forcing the shear layer at the first subharmonic frequency ($f = 2930$). The maximum increase in dispersion is approximately from 0.3 to 0.45. What makes this change perhaps more significant is not so much its magnitude, but the fact that it is produced by a forcing amplitude of only 2%. The forcing at the second subharmonic ($f = 1465$ Hz) does not show any discernible effect on droplet dispersion. The forcing at the natural instability frequency enhances droplet dispersion in the initial part of the shear layer and then decreases dispersion farther downstream. This seems to be an important result with the implication that forcing the shear layer at its natural instability frequency may strengthen the roll-up process, but delays the vortex pairings, which actually decreases droplet dispersion farther downstream. This is qualitatively in agreement with the results of Korczak and Wessel,¹² which indicate that forcing at the most dominant frequency causes faster growth of the mixing layer at the initial length and slower growth farther downstream.

Figure 6b shows the effect of the forcing amplitude on droplet dispersion. As the forcing amplitude is increased, it causes an increasingly greater enhancement in droplet dispersion compared to the unforced shear layer. However, the gain in dispersion seems to saturate for a forcing amplitude

above 2%. In other words, the forcing amplitude of about 0.02 appears to be optimum for enhanced droplet dispersion. This is partially consistent with the experimental results of Oster and Wgnanski,⁹ where it is shown that the small amplitude forcing of the shear layer tends to increase its spreading rate, but at larger amplitude, the shear layer resonates with the imposed oscillation.

Another way to demonstrate the effect of forcing on droplet dispersion is to plot the normalized dispersion function¹⁷ $\gamma(t, N) = D(t, N)/D_g(t, N)$ for the unforced and forced shear layers. Here, D is the droplet dispersion function, and D_g is the corresponding dispersion function for gas particles. The plot of γ vs time for different forcing amplitudes, shown in Fig. 7, clearly indicates that the droplet dispersion relative to the gas particle dispersion is further enhanced by forcing the shear layer. (Here, the gas particle refers to a passive scalar which is convected at the local flow velocity.) An important implication is that the increase in droplet dispersion in a forced layer may not be entirely due to the centrifugal action of the large vortical structures. This centrifugal action⁶ is believed to be responsible for enhanced dispersion for the intermediate-size droplets in an unforced shear layer. The present results therefore imply that either the centrifugal action is strengthened or perhaps another mechanism is in play for the forced shear layer, causing further enhancement in dispersion for the intermediate-size droplets. This is, however, a speculation by the authors and should not be considered conclusive. It should also be noted that the increase in dispersion due to forcing is more significant at an earlier time, i.e., in the initial part of the shear layer.

Figure 8 shows yet another way to illustrate the effect of forcing on droplet dispersion. The normalized particle distribution, which represents the fractional number of droplets at a given location, is plotted as a function of the cross-stream

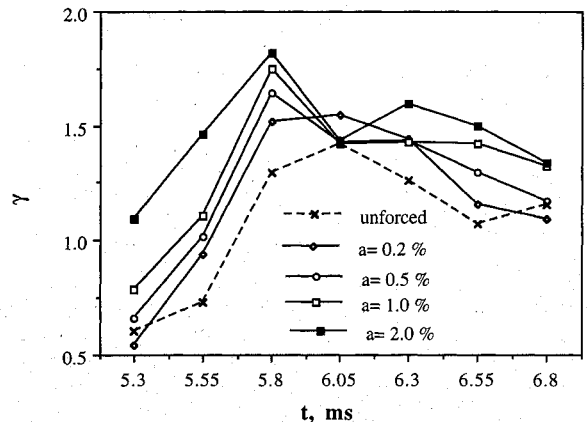


Fig. 7 Normalized droplet dispersion function vs time for different forcing amplitudes.

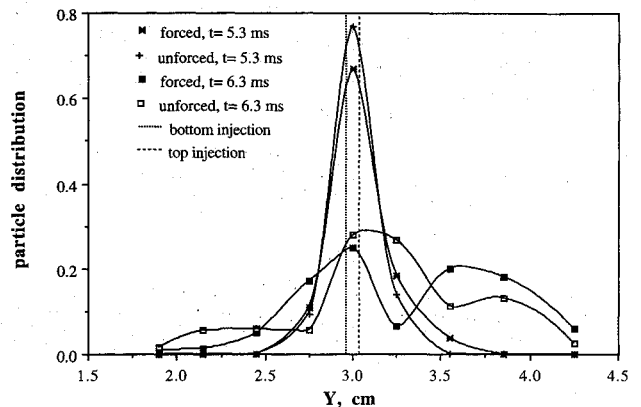


Fig. 8 Particle distribution in the cross-stream direction at different times for the unforced and forced shear layers. Diameter = 5 μm .

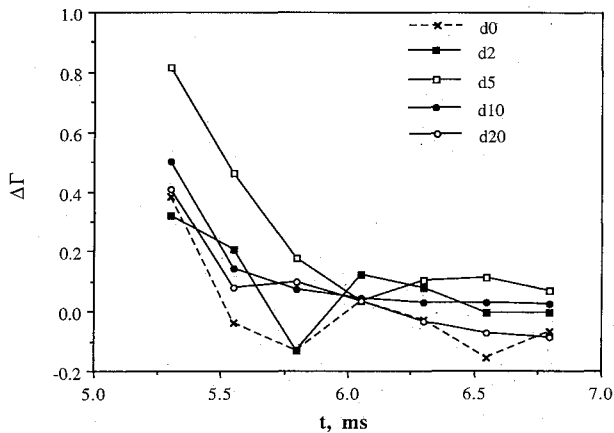


Fig. 9 Normalized dispersion function gain vs time for different droplet diameters. The forcing frequency is 2930 Hz, and the forcing amplitude = 0.01. d_0 corresponds to the fluid (tracer) particle, and d_2 , d_5 , d_{10} and d_{20} correspond to the 2-, 5-, 10-, and 20- μm droplets, respectively.

location. The results are given at $t = 5.3$ and 6.3 ms for both the forced and unforced shear layers. Note that the particles are injected, starting at $t = 4.8$ ms, from cross-stream locations between $2.96 < Y_o < 3.04$ cm; the region marked by two broken lines. Without dispersion, all the particles would maintain a value of unity there and zero outside. Due to dispersion, however, the distribution curve becomes increasingly broader with a lower peak. The important observation from Fig. 8 is that there is higher droplet dispersion, indicated by a lower peak and a broader distribution curve, for the forced shear layer compared to that for the unforced layer. Another noteworthy observation is that droplet dispersion is asymmetric. Since the initial distribution is symmetric and becomes asymmetric later with more particles on the slow side, the droplets injected in the faster side of the mixing layer ($Y_o < 3.0$ cm) are dispersed more than those injected in the slower side of the mixing layer ($Y_o > 3.0$ cm). This asymmetry in dispersion provides further evidence of asymmetric entrainment in the shear layer, observed experimentally by Koochesfahani et al.¹⁵ and numerically by Grinstein et al.,¹² Korczak and Wessel,¹⁰ and Aggarwal et al.¹⁸ A very elegant discussion of asymmetric entrainment is also given by Dimotakis.²⁵

As a final part of this study, an attempt is made to quantify the droplet dispersion gain due to forcing for different droplet diameters. The results are shown in Fig. 9, where $\Delta\Gamma$ is plotted as a function of time; $\Delta\Gamma$ is defined as the change in the dispersion function due to forcing normalized by the dispersion function for the unforced shear layer. The important observation is that the droplet dispersion may be significantly enhanced, especially in the initial part of the shear layer, by forcing the shear layer at its subharmonic frequency. The percentage gain appears to be greater for smaller droplets. It is again noteworthy that the forcing causes a disproportionately larger dispersion gain for the intermediate-size droplets compared to that for the gas particles, as discussed earlier.

Conclusions

A large eddy simulation model is used to investigate the effects of periodic forcing on the dynamics and dispersion of droplets in a spatially developing transitional shear layer. The spectral analysis of the axial velocity histories at selected spatial locations in the forced shear layer is used to obtain the needed information about the natural instability frequency and its subharmonics. The effects of forcing frequency and amplitude on droplet dispersion are then studied. The important conclusions are as follows:

1) The droplet dispersion can be significantly enhanced by a periodic forcing of the shear layer. The optimum forcing

frequency for enhanced dispersion corresponds to the first merging frequency or the first subharmonic of the fundamental frequency of the shear layer. The optimum forcing amplitude appears to be about 2%. The gain in dispersion seems to saturate, as the forcing amplitude is increased above this value.

2) The gain in dispersion for the intermediate-size droplets appears to be greater compared to that for the gas particles. This may have an important implication in that either the centrifugal mechanism,⁶ discussed earlier, is strengthened, or another mechanism is also in play for the forced shear layer. However, this observation is based on a limited set of numerical experiments, and cannot be considered entirely conclusive.

3) The present results are consistent with the previous experimental⁴ and numerical¹¹ result, which indicate that forcing at the subharmonic mode enhances the spatial growth of the layer, while forcing at the fundamental mode reduces the growth rate.

4) The influence of forcing seems to be confined to the initial region of the shear layer. This may, however, be quite significant in practical applications, where enhanced dispersion and mixing are especially more desirable in the initial region of the mixing layer. For example, in spray combustion applications, an increased dispersion in this region would mean that the droplets would get to the hot regions faster leading to enhanced vaporization and mixing.

As a concluding remark, it should be mentioned that due to some pioneering experimental studies,⁴ there is enough evidence to indicate that the shear layer growth and entrainment can be manipulated by forcing the shear layer at its subharmonic frequencies. The present study provides another confirmation. In addition, it demonstrates that the effect of forcing at a subharmonic frequency can be extended to enhance the dispersion characteristic of particles injected into the forced shear layer. A confirmation of this result is provided by two recent experimental studies,^{26,27} where it is shown that the droplet dispersion behavior can be significantly modified by external forcing.

Acknowledgments

This work has been supported by Air Force Office of Scientific Research through the Wright Laboratory, Aero-Propulsion Directorate of Wright-Patterson Air Force Base, Ohio. Julian Tishkoff is the Program Manager. The calculations were performed on Cray-YMP at the National Center for Supercomputing Applications at UIUC. Many stimulating discussions with K. Kailasanath and F. Grinstein, both at Naval Research Laboratory, Washington, D.C. are highly appreciated.

References

- ¹Brown, G. L., and Roshko, A., "On Density Effects and Large Structures in Turbulent Mixing Layers," *Journal of Fluid Mechanics*, Vol. 64, 1974, pp. 775-816.
- ²Winant, C. D., and Browand, F. K., "Vortex Pairing: The Mechanism of Turbulent Mixing-Layer at Moderate Reynolds Number," *Journal of Fluid Mechanics*, Vol. 63, 1974, pp. 237-255.
- ³Dimotakis, P. E., and Brown, G. L., "The Mixing Layer at High Reynolds Number: Large Structure Dynamics and Entrainment," *Journal of Fluid Mechanics*, Vol. 78, 1976, pp. 535-560.
- ⁴Ho, C. M., and Huerre, P., "Perturbed Free Shear Layers," *Annual Review of Fluid Mechanics*, Vol. 16, 1984, pp. 365-424.
- ⁵Corcos, G. M., and Sherman, F. S., "The Mixing Layer: Deterministic Models of a Turbulent Flow, Part 2, The Origin of the Three-Dimensional Motion," *Journal of Fluid Mechanics*, Vol. 139, 1984, pp. 29-65.
- ⁶Crowe, C. T., Chung, J. N., and Troutt, T. R., "Particle Mixing in Free Shear Layers," *Progress in Energy and Combustion Science*, Vol. 14, 1988, pp. 171-194.
- ⁷Lazaro, B. J., and Lasheras, J. C., "Particle Dispersion in a Turbulent, Plane, Free Shear Layer," *Physics of Fluids A*, Vol. 1, No. 6, 1989, pp. 1035-1044.

⁸Ho, C.-M., and Huang, L.-S., "Subharmonic and Vortex Merging in Mixing Layers," *Journal of Fluid Mechanics*, Vol. 119, 1982, pp. 443-473.

⁹Oster, D., and Wagnanski, I., "The Forced Mixing Layer Between Two Parallel Streams," *Journal of Fluid Mechanics*, Vol. 123, 1982, pp. 91-130.

¹⁰Korczak, K. Z., and Wessel, R. A., "Mixing Control in a Plane Shear Layer," *AIAA Journal*, Vol. 27, No. 12, 1989, pp. 1744-1751.

¹¹Ghoniem, A. F., and Ng, K. K., "Numerical Study of the Dynamics of a Forced Shear Layer," *Physics of Fluids*, Vol. 28, No. 6, 1987, pp. 706-721.

¹²Grinstein, F. F., Oran, E. S., and Boris, J. P., "Numerical Simulations of Asymmetric Mixing in Planar Shear Flows," *Journal of Fluid Mechanics*, Vol. 165, 1986, pp. 201-220.

¹³Grinstein, F. F., Hussain, F., and Oran, E. S., "Vortex-Ring Dynamics in a Transitional Subsonic Free Jet," *European Journal of Mechanics, B/Fluids*, Vol. 9, No. 6, 1990, pp. 499-525.

¹⁴Davis, R. W., and Moore, E. F., "A Numerical Study of Vortex Merging in Mixing Layers," *Physics of Fluids*, Vol. 28, No. 1, 1985, pp. 1626-1635.

¹⁵Koochesfahani, M. M., Dimotakis, P. E., and Broadwell, J. E., "A Flip Experiment in a Chemically Reacting Turbulent Mixing Layer," *AIAA Journal*, Vol. 23, No. 5, 1985, pp. 1191-1194.

¹⁶Chein, R., and Chung, J. N., "Effects of Vortex Pairing on Particle Dispersion in Turbulent Shear Flows," *International Journal of Multiphase Flows*, Vol. 13, No. 6, 1987, pp. 785-802.

¹⁷Chung, J. N., and Troutt, T. R., "Simulation of Particle Dispersion in an Axisymmetric Jet," *Journal of Fluid Mechanics*, Vol. 186, 1988, pp. 199-222.

¹⁸Aggarwal, S. K., Chen, G., Yapo, Y., Grinstein, F. F., and Kailasanath, K., "Numerical Simulation of Particle Dynamics in Planar Shear Layers," AIAA Paper 92-0109, Jan. 1992; also *Computers and Fluids* (submitted for publication).

¹⁹Faeth, G. M., "Mixing Transport and Combustion in Sprays," *Progress in Energy and Combustion Science*, Vol. 13, 1987, pp. 293-320.

²⁰Grinstein, F. F., Oran, E. S., and Boris, J. P., "Pressure Field, Feedback, and Global Instabilities of Subsonic Spatially Developing Mixing Layer," *Physics of Fluids A*, Vol. 3, 1991, pp. 2401-2409.

²¹Boris, J. P., Grinstein, F. F., Oran, E. S., and Kolbe, R. L., "New Insights into Large Eddy Simulation," Naval Research Lab. Rept. NRL/MR/4400-92-6979, April 1992.

²²Kung, L., "Numerical Simulations of Forced and Unforced Shear Layers," M.S. Thesis, Dept. of Mechanical Engineering, University of Illinois at Chicago, Chicago, IL, 1992.

²³Hussain, Z. D., and Hussain, A. K. M. F., "Natural Instability of Free Shear Layer," *AIAA Journal*, Vol. 21, No. 11, 1983, pp. 1512-1518.

²⁴Clift, R., Grace, J. R., and Weber, M. E., "Bubbles, Drops, and Particles," Academic Press, New York, 1978.

²⁵Dimotakis, P. E., "Two-Dimensional Shear Layer Entrainment," *AIAA Journal*, Vol. 24, No. 10, 1986, pp. 1791-1796.

²⁶Lazaro, B. J., and Lasheras, J. C., "Particle Dispersion in the Developing Free Shear Layer. Part 2. Forced Flow," *Journal of Fluid Mechanics*, Vol. 235, 1992, pp. 179-221.

²⁷Longmire, E. K., and Eaton, J. K., "Structure of a Particle-Laden Round Jet," *Journal of Fluid Mechanics*, Vol. 235, 1992, pp. 217-257.

AEROSPELL™

To order

Order reference:

WP/DISK-1 (WordPerfect/DOS)

MW/DISK-2 (Microsoft Word/Macintosh)

by phone, call 800/682-2422, or

by FAX, 301/843-0159

For mail orders:

American Institute of
Aeronautics and Astronautics
Publications Customer Service
9 Jay Gould Court, PO Box 753
Waldorf, MD 20604

\$50.00 per copy

Postage and handling charges:

1-4 items \$4.75 (\$25.00 overseas)

5-15 items \$12.00 (\$42.00 overseas)

All orders must be prepaid. Checks payable to AIAA, purchase orders (minimum \$100), or credit cards (VISA, MasterCard, American Express, Diners Club)

For bulk orders or site licenses, call Adam Bernacki, AIAA, 212/315-0134.

Add 5500+

new technical aerospace terms to your WordPerfect® or Microsoft Word® spell-checkers

Based on terminology in AIAA's Aerospace Database, **AeroSpell™** integrates easily into your existing spell checker, automatically helps produce more accurate documents, and saves you valuable search time.

The word list includes aerospace, chemical, and engineering terminology, common scientific and technical abbreviations, proper names, and much more.

Package includes 5.25" and 3.5" HD diskettes and installation instructions for **WordPerfect®** and **WordPerfect® for Windows** (DOS) or **Microsoft Word®** (Macintosh).

AIAA
American Institute of
Aeronautics and Astronautics